

# Can Machine Learning Uncover Insights into Vehicle Travel Demand from Our Built Environment?

Zixun Huang<sup>a,\*</sup>, Hao Zheng<sup>b</sup>

<sup>a</sup>University of California at Berkeley, CA, USA  
<sup>b</sup>City University of Hong Kong, Hong Kong, China

---

## Abstract

In this paper, we propose a machine learning-based approach to address the lack of ability for designers to optimize urban land use planning from the perspective of vehicle travel demand. Research shows that our computational model can help designers quickly obtain feedback on the vehicle travel demand, which includes its total amount and temporal distribution based on the urban function distribution designed by the designers. It also assists in design optimization and evaluation of the urban function distribution from the perspective of vehicle travel. We obtain the city function distribution information and vehicle hours traveled (VHT) information by collecting the city point-of-interest (POI) data and online vehicle data. The artificial neural networks (ANNs) with the best performance in prediction are selected. By using data sets collected in different regions for mutual prediction and remapping the predictions onto a map for visualization, we evaluate the extent to which the computational model sees use across regions in an attempt to reduce the workload of future urban researchers. Finally, we demonstrate the application of the computational model to help designers obtain feedback on vehicle travel demand in the built environment and combine it with genetic algorithms to optimize the current state of the urban environment to provide recommendations to designers.

*Keywords:*

Vehicle Travel Demand; Urban Data Mining; Land Use Optimization; Neural Networks

---

## 1. Introduction

### 1.1. Background

A significant number of empirical studies demonstrate the interdependence between land use and local vehicle travel demand through household surveys (Cervero, 1991, 1996; Cervero and Duncan, 2003). For example, researchers have shown that mixed-use development (MXD) promote the alternative role of non-motorized travel choices such as walking and cycling (Cervero and Kockelman, 1997; Maria Kockelman, 1997; Park et al., 2018), and high density facilitates the use and development of public transit mode (Cervero, 1994; Dunphy and Fisher, 1996). And recent researchers have revealed that both the abundance and spatial configuration of urban land use are correlated with traffic congestion (Wang and Debbage, 2021).

Management of traffic resources using an urban design perspective proves to be feasible and effective (Cervero and Kockelman, 1997; McNally and Kulkarni, 1997). These urban studies receive significant attention to quantify and measure travel behavior, built environment, and the correlation between the two (Song et al., 2013; Ewing and Cervero, 2001; Clifton et al., 2008; Ewing and Cervero, 2010). To encourage efficient utilization of traffic resources and improve the relation between traffic supply and demand, there exists tools for policymakers

and urban designers to consider involving traffic analysis and prediction from the perspective of land use (Wachs, 1989).

### 1.2. Problem Statement

However, deficiencies and omissions in past studies hamper more detailed conclusions that help urban designers determine the relationship between vehicle travel demand and urban functions and then to carry out a better urban design.

The prevailing measurement methods of urban environment used in these studies omit specific information regarding urban function ratio, thus failing to provide urban designers with more detailed references. The entropy index, for example, illustrates this shortcoming. Different proportions of urban functions may produce the same entropy value, and the highest one hinders the designers in crafting the most appropriate LMU strategy (Song et al., 2013). Occasionally, the variances in research subjects, such as neighborhoods, are consolidated into a single categorical variable with a concomitant loss of information (Ewing and Cervero, 2001), including but not limited to function distribution information. However, some researchers have studied the influence of specific urban functions such as offices, residences, retail and transit on vehicle travel behaviors and demonstrated the impact of specific urban functions on transportation travel (Cervero and Duncan, 2006; Systematics et al., 1994; Choi et al., 2021).

Limited information and dimensionality of survey data left a dearth of detail on the impact of urban function distribution on

---

\*Corresponding author.

Email address: zixun@berkeley.edu (Zixun Huang)

local vehicle travel demand temporal distribution. Peak congestion serves as a major challenge for urban traffic networks with limited bearing capacity. Average distribution of the traffic in time can help share the traffic pressure (Loudon et al., 1988; Downs, 2005; Shallal and Khan, 1980). Cervero suggested in his early research that trips tend to be more evenly distributed throughout day and week in a more mixed-function community (Cervero, 1996, 1989). While most literature in this field mainly focus on the impact of land use on the total amount of traffic, such as vehicle miles traveled (VMT) and vehicle hours traveled (VHT), few studies focused on and made conclusions the relationship between urban land use and temporal distribution of vehicle travel demand.

Empirical evidence struggles to be repeated in new study areas, cultures, and eras. Traditional travel behavior modeling relies on labor-intensive, high-cost, and time-consuming data collection methods such as American Household Surveys and local travel surveys that make large scale, in-time analysis extremely difficult to achieve (Li et al., 2020). Past empirical evidence on the transportation impact description of built environments rendered itself inconsistent (Cervero, 1996; Cervero and Duncan, 2006) and unsuitable for comparison due to lacking reliable standard error estimates from individual studies (Ewing and Cervero, 2010). For instance, Cervero utilized building height as a proxy for employment density (Cervero, 1991) while others use gross population density (Dunphy and Fisher, 1996) to measure a similar problem. Thus, designers often spend high labor costs to verify the practical effects of the empirical conclusions in a different region.

In summary, researches based on the traditional survey method have provided abundant conclusions of built environment factor, including but not limited to local density, diversity, and single-function distribution, and its impact on travel behavior. Designers find inspiration based on these findings to construct a better planning decision. However, these research methods lack further detail regarding the spatial patterns of urban functions as well as the temporal patterns of vehicle travel demand. They also fail to illustrate the relationship between them and produce viable conclusions in other different areas.

### 1.3. Data-driven and Machine Learning Based Urban Study

With the development of artificial intelligence (AI) and urban information management, urban designers acquire opportunities to enhance traditional workflow and analyze in detail the traditional urban problem (i.e., how urban function distribution affects vehicle travel demand) from integrated quantitative and qualitative perspectives. Rapid advancement in information and communications technology has facilitated a generation of data capturing human movements and daily activities (Li et al., 2020; Chauhan et al., 2016). An increasing number of urban researchers have adopted ubiquitous urban data collected in real-time (Kang et al., 2020; Shen and Karimi, 2016; Gervasoni et al., 2016; Yuan et al., 2012) to quantify and describe urban patterns and processes. Additionally, machine learning (ML) related algorithms have been used to create models that perform predictive functions in data-driven urban study (Nosratabadi et al., 2019; Souza et al., 2019). The consensus states

that ubiquitous urban data combined with ML technology bears tremendous potential in the field of urban studies and smart city solutions (Nosratabadi et al., 2019; Hancke et al., 2013; Ibrahim et al., 2020; Hadjimichael et al., 2016; Youssef et al., 2020).

When applied, ML algorithms are capable of automating urban tasks such as land use and land cover (LULC) mapping and zoning (Demir et al., 2018; Kandrika and Roy, 2008); predicting future urban evolution (Grekousis et al., 2013); mapping residential density patterns jointly with multi-temporal Landsat data (McCauley and Goetz\*, 2004); discovering function regions with human mobility and points of interest (POI) data (Yuan et al., 2012); identifying land-use type based on temporal traffic patterns with taxi data (Liu et al., 2012); automatically evaluating the urban visual environment in a large scale (Liu et al., 2017); estimating health outcomes at a neighborhood scale (Feng and Jiao, 2021).

Related research on the application of ML in travel behavior includes applying decision tree (DT) induction (Loh, 2011) to predict transport mode (Wets et al., 2000) and route choice (Yamamoto et al., 2002; Arentze et al., 2000). ML can also be used for exploring the relationship between ride-sourcing services and vehicle ownership (Sabouri et al., 2020). Deep learning approaches to predict the short-term demand of bike-sharing FFBS with weather and air quality data (Bao et al., 2019) and to develop a prediction system for real-time parking in smart cities (Vlahogianni et al., 2016).

### 1.4. Objective

This research aims to develop a method capable of creating a computational model that maps detailed built environment information into vehicle travel demand information including temporal distribution and total amount. Such a model, therefore, aids urban designers in receiving feedback quickly and decision-makers in optimizing the allocation of resources to achieve a balance between traffic and other urban purposes like residence, commerce, industry, and infrastructure.

This research combines travel behavior data and urban function distribution to generate a machine learning model that offers vehicle travel demand prediction. We developed an ML model that learns experiences from urban data to help designers automate detailed traffic demand judgments in a certain area of a given city. Regarding the problem statement, the prediction model of this study is based on three setups.

1. An input feature about local built environment defined as a ratio between urban functions in the region of study instead of a single categorical variable or a measure of land use mix;
2. An output feature about travel behavior defined as the average daily quantity and temporal distribution of vehicle travel demand in study region instead of VMT or VHT;
3. Commonly used open-source urban data utilized as training data sets for the prediction model to examine the cost efficiency of applying this research method to different cultural areas.

This research aspires to use a computer, which inputs detailed urban function distributional information to the program,

to predict the average daily quantity and temporal distribution of vehicle travel demand of a given local area. The temporal distribution image of vehicle travel demand becomes an output regarded as a reference to adjusting urban function distribution within the area. Then, the ML model is reused to verify the adjusted urban function distribution and determine whether the revision achieves a purpose that makes more rational use of traffic resources. Furthermore, urban function composition information can be iteratively optimized by combining the prediction model with a genetic algorithm.

## 2. Methodology

This section explains the method, primarily regarding data preparing, sampling, and model training. Figure 1 shows a general introduction to the production of a more detailed forecast of vehicle travel demand. First, data about the built environment and the travel demand should be collected and quantified through a web crawling and data cleaning process. After that, the data-set is redivided into a series of data samples based on geographic location. Subsequently, forecasting models such as Artificial Neural Networks map the relationship between the urban environment and vehicle travel demand based on the processed samples. The prediction models should serve as a guide for designers and decision-makers to interpret environmental information and meet the crowd travel demands.

### 2.1. Data Preparing and Feature Sample Rule

To describe the urban local function environment in detail, points of interest (POI) are selected as elements that form our living environment. Urban function density and mix in local areas of different scales, such as in function zones (Yao et al., 2017); in neighborhoods (Yue et al., 2017); in living areas (Liu et al., 2020); in 1km buffers (Zhao et al., 2018); and at the census tract level (Maharana and Nsoesie, 2018), are measured as the quantitative relationship between POI. In this study, we describe our urban function environment in the following way: the total number of POI types defined as  $k$ ; the amount of POI type  $j$  in a local area  $Z$  denoted as  $x_Z^j$ ; the density of all urban function types within the district  $Z$  measured by proxy as  $X_Z = \sum_{j=1}^k x_Z^j$ ; and the percentage of the urban function  $j$  measured as  $p_Z^j = \frac{x_Z^j}{X_Z}$ . It follows that  $\sum_{j=1}^k p_Z^j = 1$ .

To obtain an urban function spatial distribution containing latitudinal and longitudinal information, we choose AutoNavi as the data source, which is a Chinese web mapping, navigation and location-based services provider. Based on POI code table provided by AutoNavi, urban functions are divided into 16 categories (Table 8).

According to the API user guide, city code and POI code are initially selected as main crawling input parameters. However, we discovered that POI in each category are limited to 900 points with city code as a parameter input, which causes a sparse urban function distribution and leads to unreasonable equaling of different POI types. The urban function environment cannot be described accurately in this situation. To solve this problem, the entire target area is divided into smaller equal

parts for finer crawling to acquire information on the built environment that more accurately reflects reality. The POI information in each part is then captured and categorized by POI types (Figure 2).

After obtaining the detailed urban function distribution data, we sample the whole urban area uniformly for input features for machine learning later. The feature sampling rule follow as such (Figure 3):

1. A buffer area with a radius of 1 km, a standard unit of measurement in urban researches (Zhao et al., 2018; Frank et al., 2004, 2005; Sallis et al., 2016) regarding the relationship between land use and travel behavior, defined as a basic sampling unit;
2. The whole area of interest sampled every 200 m (i.e., general land block scale);
3. A sampling unit defined as region  $Z$ , the proportion of urban functions  $p_Z^j$  and density  $X_Z$ , and measured as urban environment features of this unit. In addition, we normalize the density feature of each sample. The maximum density proxy value of all cells is denoted as  $D$ , and the normalized density value of each sample is redefined as  $X_Z^* = \frac{X_Z}{D}$ . The total number of samples is defined as  $n$ . For sample  $Z$  ( $Z=1-n$ ), the final 17 built environment features obtained by this sampling method are  $X_Z^*$  and  $p_Z^j$  ( $j=1-16$ ), which describe the whole density of urban functions and detailed proportion of 16 urban functions in the study sample  $Z$ .

Pertaining to vehicle travel demand data, this research adopts open-source data. Taxi as a door-to-door, all-weather way of travel becomes the subject of study. Vehicle travel demand in a certain place can be represented by taxi orders or vehicle hours traveled (VHT) generated by those orders. The regression model developed by Liu (Liu et al., 2020) shows strong links between demand for taxis and urban form characteristics. For a large body of emergent data related to travel behavior (Liu et al., 2012; Davis et al., 2016; Tong et al., 2017; Zhang et al., 2017), taxi data proves to be an excellent option because of its ease of acquisition and large data size. Valuable actual and general data are generated along due to a mass of real behaviors. Moreover, vehicle hours traveled (VHT), which has been proven significant in environment research, is ultimately selected as the fundamental travel variable as a result of convincing, prior empirical studies by Ewing and Cervero about processing travel behavior data. (Ewing and Cervero, 2001).

Traffic order data are distributed evenly to each day and then divided into 24 intervals based on the time of order. Subsequently, these data are sampled in the same way mentioned above. In addition, information on hours traveled is extracted from the orders to describe exact travel demand based on Cervero's previous research. Therefore, each piece of order is bound with an additional weight coefficient representing VHT generated by order data. For a geographic unit  $Z$  sampled, the average daily order is counted as  $c_Z = \sum VHT$ . The orders between  $i$  o'clock and  $i + 1$  o'clock are formulated as  $c_Z^i$  ( $i=0-23$ ). The order distribution ratio in each interval is marked as

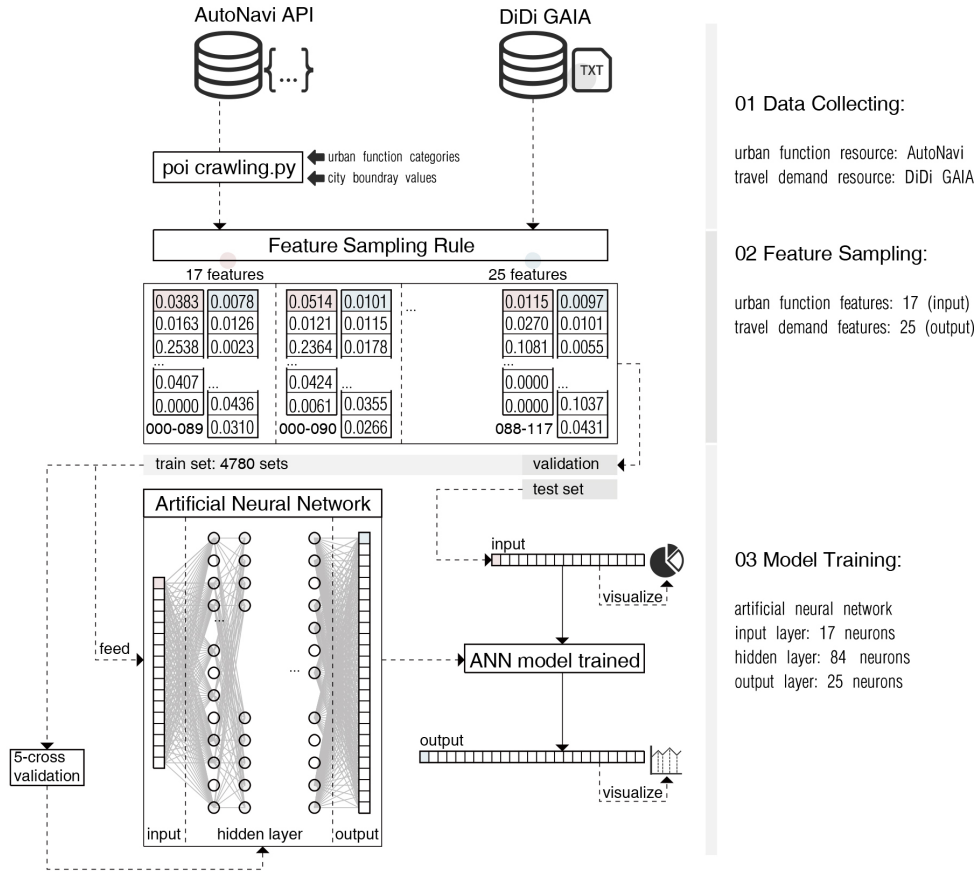


Figure 1: Data pre-processing and neural network training method.

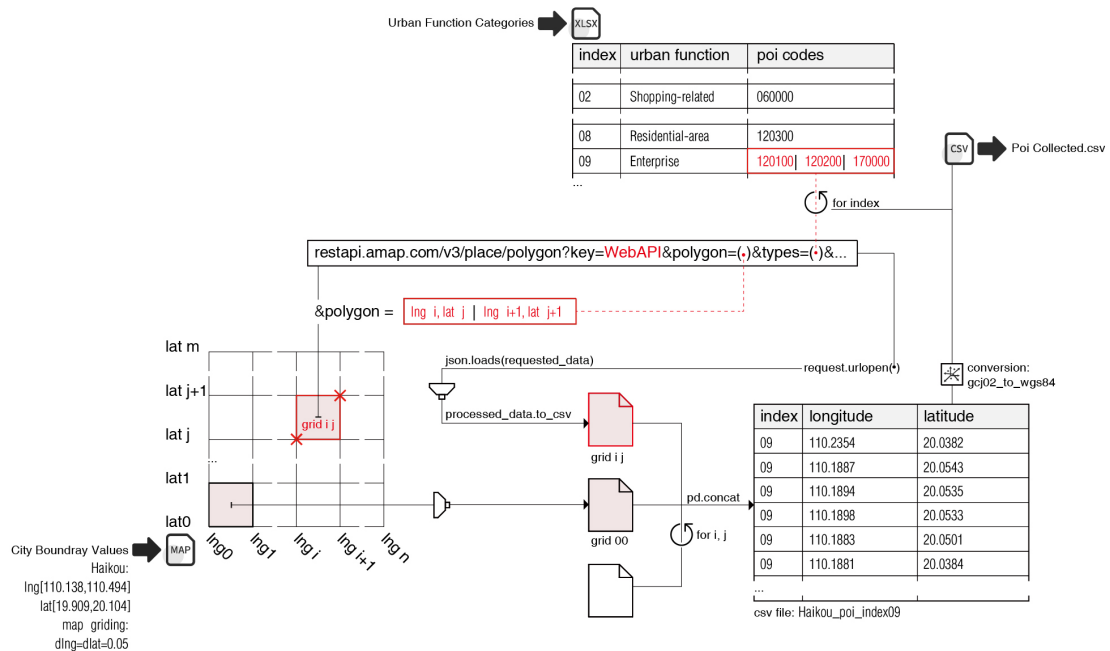


Figure 2: The process of built environment information crawling

$q_Z^i = \frac{c_Z^i}{c_Z}$ . Therefore, it follows that  $\sum_{i=0}^{23} q_Z^i = 1$ ; For sample Z, method are normalized  $c_Z^*$  and  $q_Z^i$  ( $i=0-23$ ), which describe the final 25 travel demand features obtained by this sampling whole density of travel demands and detailed VHT distribution

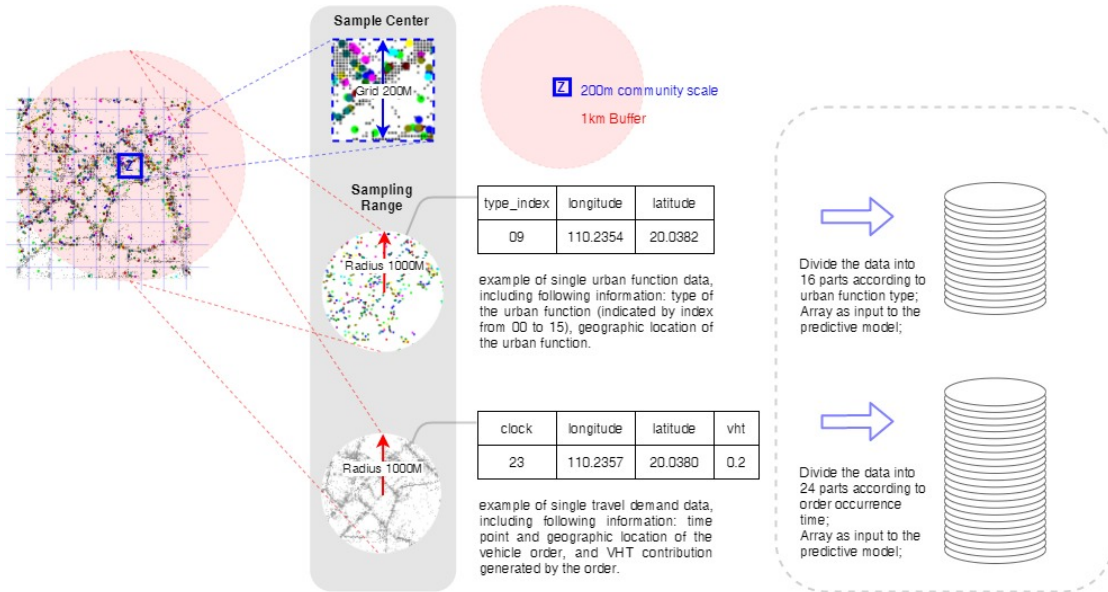


Figure 3: The flow chart of the feature sampling rule

throughout a day in study sample Z.

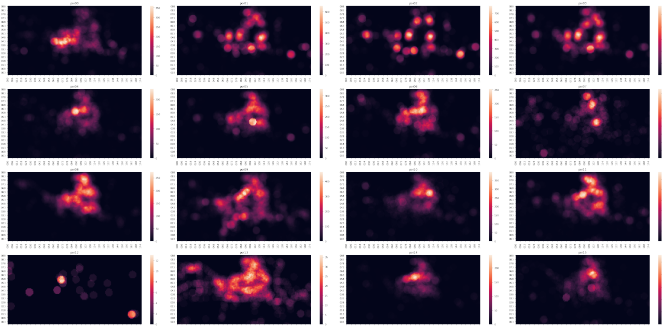


Figure 4: Heat distribution maps of 16 kinds of urban functions (sorted by Table 8). For each map, the brighter grid region contains the more function points.

## 2.2. Study Area

A port city in China named Haikou recently approved international tourism island construction. Consequently, a rapid increase of vehicle ownership and urban road traffic gradually became obstacles restricting the development of its social economy. The high sand content due to Haikou's special geology poses the risks of surface subsidence and seawater back-up. Thus, it is difficult to establish a subway system as public transportation to relieve the pressure of traffic.

A total of 65680 POI data of Haikou is obtained through a Python program called API provided by AutoNavi. A month's amount of taxi order data in Haikou totaling 1,809,517 is provided by Didi Chuxing GAIA Initiative, an open-source data set. According to feature sampling rules, 15664 sample units were collected from the location of (110.138, 19.909) to (110.494, 20.104) in the GCJ02 coordinate system. Python is used to grid the geographical scope of Haikou and to calculate 17 built environment features and 25 travel demand features for each grid in this process.

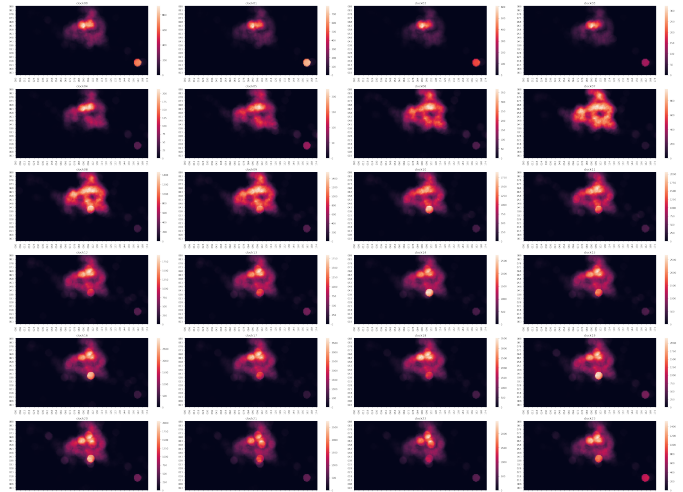


Figure 5: Heat distribution maps of 24 segments of VHT (from 0 o'clock to 23 o'clock). For each map, the brighter grid area represents the higher total VHT value compared with other grids.

Only 5991 valid units are reserved for neural network training after data cleaning operations to ensure that all samples contain valid built environment information and effective travel requirements. Samples that fail to contain any POI information or exceed one taxi order per hour on average in its radiation buffer are excluded.

In addition, (Figure 4) and (Figure 5) illustrate the urban function and travel data demand respectively collected in Haikou. Although not the focus of this research, they help us better understand the characteristics of the site in order to evaluate the prediction results of the computational model. Through these two sets of maps, we macroscopically see the distribution of regional centers of different functions and how active vehicle travel demand flows over time.

### 2.3. Neural Network Training and Accuracy Definition

This research endeavors to formulate computational models that predict vehicle travel demand that also include information about traffic temporal distribution with respect to the density and composition of urban functions. The prediction models should therefore help designers adjust and optimize their urban planning.

ANNs, Random Forest (RF), and Support Vector Machine (SVM) are chosen as the algorithms to obtain a computational model applicable to this study. ANN-based models, in particular, utilize Back-Propagation (BP), which fine-tune the weights of neurons to find practically accurate solutions for formulated problems and phenomena only understandable through experimental data and field observations (Basheer and Hajmeer, 2000). They fulfill the problem of connections between our built environment and vehicle travel demand.

Understanding the complexity in both forecasting total demand and acquiring detailed information, we constructed different structures of neural networks referred to as network T and D. The built environment information processed by feature sampling rules can be initially set as 17 input neurons with values ranging from 0 to 1, indicating a proportion of 16 urban functions and a normalized density compared with the densest area. As for the output structures, the number of neurons is determined by the number of parameters needed to predict different network structures. For network T, total vehicle travel demand is set as one output neuron with a value from 0 to 1, indicating the normalized total demand compared with the most active area. For network D, detailed temporal distribution is set as 24 output neurons with a value from 0 to 1, indicating a 24-hr VHT distribution ratio. In addition, sigmoid function and mean squared error (MSE) are selected as activation and loss functions when training our neural networks.

The number of hidden layers and neurons therein should also be defined. Based on the literature (Karsoliya, 2012) and actual tests, suitable results are obtained when the number of neurons of each hidden layer is 36 for network T and 82 for D. Five-fold cross-validation tests are employed to find neural network structures catering to the complexity of our study problem. Accuracy functions are customized to ascertain the loss function and help us better evaluate the accuracy of the outputs.

Equation 1 is used to evaluate the prediction accuracy of the vehicle travel demand density (the total VHT amount all over the day). In this formula, we take the absolute value of the difference between the predicted value of the normalized local total amount of VHT and its ground-truth value as the error value.

$$Accuracy = 1 - \frac{|groundtruth_{allday} - prediction_{allday}|}{groundtruth_{allday}} \quad (1)$$

Equation 2 evaluates the prediction accuracy of detailed VHT temporal distribution. With it, we take the sum of the absolute value of the difference between the predicted values of VHT per hour and their ground truth value as error.

$$Accuracy = 1 - \sum_{clock=0}^{23} |groundtruth_{clock} - prediction_{clock}| \quad (2)$$

We tested our neural networks on parts of the Haikou region using the processed environment information as the inputs and the processed demand data as the outputs. A total of 898 feature samples are divided into 5 parts, four for training and one for validation. Table 1 presents the median accuracy of neural networks with different layer sizes in the fivefold cross-validation test. We also compared our artificial neural networks with other types of machine learning models such as the RF and Linear SVM. ANN noticeably achieves higher accuracy at least for predictions in the local area with randomly distributed samples. Meanwhile, the artificial neural network T with 7 layer-size sports the highest accuracy in the vehicle travel demand prediction of local total demand while the neural network D with 8 layers is most accurate in the demand prediction of detailed temporal distribution. As a result, the neural networks with 7 layer-size and 8 layer-size are chosen as the preliminary settings. In addition, we used a batch size of 100 in the preliminary settings and the customized error rate (1- accuracy) with increasing epochs recorded during the experiments to help us find an appropriate number of iterations in prediction model training (Figure 6).

### 2.4. Post Process and Visualization

Using the trained model, the predictions of vehicle travel demand information are remapped into values before normalization. They respectively represent the total VHT values throughout one day and the proportions of VHT produced in 24 one-hour periods on geographic units. In addition, the prediction values are then visualized and compared with the ground truth values.

## 3. Result and Application

### 3.1. Accuracy of Training Set and Test Set

Based on feature sampling rules and the training method settings mentioned above, two forecast models at various regional scales are built and trained with different data sets. Up to 5991 valid samples, inclusive of the built environment and vehicle travel demand information, represent the whole area of Haikou. 898 samples signifying the Haikou urban area (Figure 11) are used as data sets to test the accuracy of the two neural networks. In the case of random geographic distribution, 80 percent of samples are used in the training process, and the remaining samples are used in accuracy tests.

Figure 6 and 7 present the error rates of the demand forecast models both in the urban and whole area of Haikou, showing they fall to a convergent state as the number of training iterations increases. The results plotted in the figures fulfill expectations regarding the prediction accuracy of the Haikou urban model test: 95.68% for the average total VHT throughout one day, 97.84% for the VHT temporal distribution prediction. The

ANN Structure	Median accuracy for detailed temporal distribution (%)	Median accuracy for local demand density (%)
2- Layer ANN	95.86	91.6
3- Layer ANN	96.52	93.86
4- Layer ANN	97.07	94.1
5- Layer ANN	97.57	94.81
6- Layer ANN	97.48	95.52
7- Layer ANN	97.78	<b>95.68</b>
8- Layer ANN	<b>97.84</b>	95.22
9- Layer ANN	97.57	95.1
Others	-	-
Random Forest	91.78	91.88
Linear SVR	92.96	91.61

Table 1: Five-fold cross-validation of neural networks with different numbers of layers.

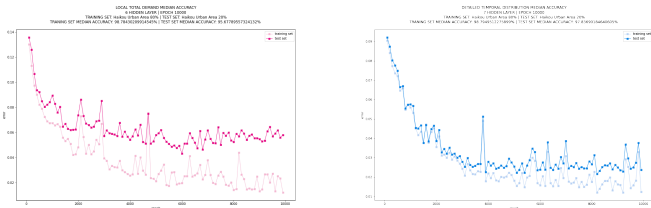


Figure 6: This figure presents the error rate variation of the prediction model in the urban area of Haikou with the number of iterations increasing. The red lines represent total VHT amount prediction error rates and the blue lines represent VHT temporal distribution prediction error rates; the bright lines represent the error rates variation in the test set, and the faded lines represent the error rates variation in the training set.

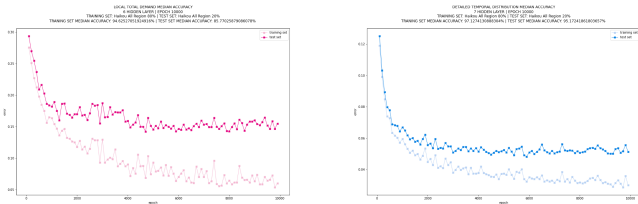


Figure 7: The same as Figure 6. This figure presents the error rate variation of the prediction model in the whole area of Haikou with the number of iterations increasing.

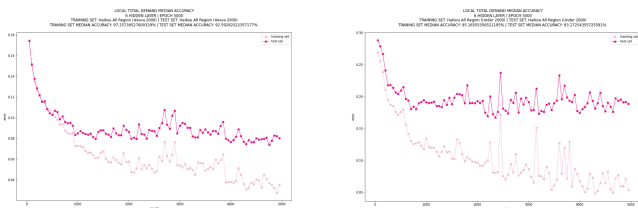


Figure 8: The prediction error rates of daily total VHT amount, Right: trained with samples having accumulated VHT of less than 2000 hours within a month, Left: trained with samples having accumulated VHT of more than 2000 hours within a month.

prediction accuracy of the Haikou all-region model test boasts an accuracy of 85.77% for the average total VHT throughout one day, 95.17% for the VHT temporal distribution prediction.

Nine samples from the all-region model test were randomly calculated, had their prediction outputs visualized, and then

compared to the ground truths. The built environment inputs and the detailed demand predictions are displayed in the table 2 and 3. The bright lines of Figure 9 present the prediction results of these instances calculated by our neural network, and the corresponding ground truths represented by the faded lines are also plotted in these figures to make a comparison (i.e., ST82, ST271, ST279, ST490, ST673, ST912, ST932, ST990, and ST1077 represent different samples from the test set, which annotate their numerical positions). Figure 10 depicts the predictions and the ground truths of total VHT throughout one day.

An accuracy of 85.77% in the average total VHT prediction of Haikou is a relatively low value when compared with the results draw from exclusively its urban area, but the prediction results seem acceptable when visualized into circle areas. Most cases with low accuracy occur in remote places that have few and random travel orders compared with those located in urban areas. An understandable reason for this discrepancy is the lack of travel orders to form a consistent and regular pattern in these samples; therefore, slight differences in absolute value lead to notable error rates as ST271 shows in figure 10.

To determine if samples with sparse travel activity cause the problem of accuracy, we roughly divided the all-region data set into two parts. One contains 3065 samples, each of which accumulated VHT of no more than 2000 hours within a month (Set-A), and the other part contains 2935 samples that each accrued VHT above 2000 hours (Set-B). Two computational models are therefore trained with these two data sets and preliminary network structure. Figure 8 plots the median error rates of both models' predictions in daily average total VHT amount. They show that convergence and overfitting of the model trained by Set-A occurred at approximately 1000 epochs, and that accuracy sits at a relatively low at 83.27%. After removing the data samples with low travel activity, the model trained with the retained data shows a higher accuracy rate of 92.59% and a stabler error fitting curve.

The results are visualized and analyzed for VHT temporal distribution predictions as well. Our calculation model sports a significant fitting effect on the detailed temporal proportion distribution of travel demand. According to the same problem above, some samples in remote places without abundant vehicle orders to produce VHT incompletely fit the truths as ST990

shows, which has an accuracy of 64.17% below the median accuracy.

In conclusion, we received satisfying median accuracy results about the neural network used to map a link between a given built environment and vehicle travel demand prediction. The detailed temporal distribution of the demand offers acceptable median accuracy as well. For total demand, despite the presence of samples with insufficient travel activities muddling their demand patterns, the magnitude of the total remains relatively correct and distinguishable from samples with significant travel activities through the visualization process. These verify the feasibility of our computational models to forecast vehicle travel demand in different periods, and these models perform better in areas with frequent human activities compared to remote ones.

### 3.2. Cross-city Experiment

With the aid of trained computational models, we successfully analyzed and judged the results of traffic demand in Haikou based on the given built environment information. However, it remains to be verified if this prediction model can be migrated across different regions. The twofold issue manifests as such: (1) whether a predictive model trained in one city can be applied to another city, and (2) whether a model trained in one part of a city can be used for the entire area. To verify the universality of the relationship between environment and vehicle travel demand and further demonstrate the applicability of our method, we trained the neural networks for different areas (Figure 11) and conducted a hybrid test. In addition, although ANNs performed best in fitting the mapping relationship in the preliminary five-fold accuracy verification test, algorithms such as RF and Linear SVR are also reconsidered while accounting for the modification in training data and test sets.

This section details the final accuracy of our prediction models in the experiments involving both the urban and whole of Haikou, Chengdu urban area, and algorithmic adjustments for better performance in multi-area applications. Data sampling and model training processes were conducted on these different areas, and the trained models are applied to the other two regions to acquire accuracy. By comparing and analyzing the median accuracy of models applied to different areas and graphing the prediction results, we determine the extent to which the prediction model can be reused.

#### 3.2.1. Aggregate Forecasting: Region Migration

First, on the topic of VHT aggregate forecasts used across regions, we applied the model trained to the center of one city and then to that of another. Secondly, the prediction values are visualized to show the effect of the computational model and compare the experimental results of different algorithms and datasets (Figure 12). The predicted total VHT for each sample is remapped to the value before normalization and translated into a color value. Brighter and warmer colors represent higher values. Sample color blocks are reassembled in the area of interest and measured onto a map in km, depicting the predicted total vehicle travel demand as a macroscopic geographic distribution to be compared to reality. In addition, the relative error

between the predicted and true values for each sample is visualized as a color value. Blacker means a higher accuracy of the prediction model whereas whiter represents a higher error value. Similarly, the error value color block is reallocated onto the map.

One model is trained in Haikou, then tested in Chengdu, and vice versa with the other (Figure 12). After comparing the prediction images generated by the different algorithms and the median accuracy of the samples, we suggest that ANNs bear the best prediction results. ANNs boast not only higher median accuracy but also generate images with prediction values closest to the real VHT distribution. The prediction results of RF have a low subdivision in the color value of VHT aggregate. The degree of subdivision and accuracy increase with the tree depth value, but the change becomes extremely subtle when depth exceeds 5. The accuracy of SVM is also not as high as ANNs, and according to the visualization of the predicted values, SVM overestimates the VHT value of samples with sparse travel activity.

The visualization of VHT generated by ANNs matches the spatial distribution trend of the real situation. To clarify, total VHT in Chengdu decreases from the lower-left outward in the predicted image, and the total VHT in Haikou aggregates laterally in the middle of the predicted map. This indicates that the prediction model for the total VHT amount works for another city whose data is completely unlearned by the artificial neural network during the training process.

However, the color value distribution tends toward average more than the real. We tested different activation functions to obtain better prediction results. The experiments show that Relu and Softmax fail to fit the training of the prediction model. The results of Tanh and Sigmoid are similar. We ultimately chose Sigmoid as the final activation function because it provides a more even distribution of color values while Tanh generates predictions with slightly lower accuracy. Under those conditions, Sigmoid brightens the darker parts of the upper left and lower right diagonal of Chengdu prediction. In the Haikou prediction image, it darkens the central area (Figure 12).

Additionally, the accuracy images of ANNs show the sample with ground truths of higher total VHT amount have darker color values (i.e., the ANNs model holds a higher prediction accuracy on that sample). However, the sample with the highest accuracy is not at the center of the city, where the highest VHT values converge, but in the outer ring, where the total VHT values are slightly lower. The black area in the accuracy plot consistently appears as a ring, and the interior contains dark gray blocks slightly brighter compared to the edges, meaning the accuracy of the ANN model first starts higher and lowers from the center of the city outward.

In general, the prediction models for VHT aggregate are migratable between different urban areas provided that ANNs use Sigmoid, possessing a median accuracy of around 75%, increasing and then decreasing from the city center outwards.

#### 3.2.2. Aggregate Forecasting: Region Expansion

However, there exists the question of applying models trained in a small-scale urban area dataset to a larger scale one.

Inputs	ST82	ST271	ST279	ST490	ST673	ST912	ST932	ST990	ST1077
poi 00	6.94%	8.62%	1.38%	4.32%	3.57%	7.82%	10.22%	2.38%	3.54%
poi 01	14.30%	10.92%	17.59%	9.31%	5.95%	8.64%	14.06%	7.14%	9.60%
poi 02	10.93%	7.47%	19.66%	6.06%	16.67%	31.48%	9.74%	26.19%	11.11%
poi 03	17.87%	8.62%	15.17%	9.31%	3.57%	4.73%	17.57%	11.90%	13.13%
poi 04	2.94%	3.45%	6.55%	8.59%	0.00%	1.03%	1.60%	0.00%	2.02%
poi 05	6.87%	5.17%	1.03%	5.31%	2.38%	1.03%	4.47%	0.00%	2.53%
poi 06	6.24%	0.57%	1.38%	8.63%	1.19%	1.65%	3.51%	7.14%	5.56%
poi 07	0.56%	1.15%	1.72%	0.44%	0.00%	0.82%	0.32%	0.00%	0.51%
poi 08	6.24%	1.72%	1.38%	6.26%	0.00%	2.47%	5.91%	0.00%	13.13%
poi 09	8.69%	32.76%	14.48%	13.66%	33.33%	20.58%	11.50%	11.90%	7.58%
poi 10	7.85%	5.17%	7.93%	5.23%	10.71%	6.58%	7.03%	2.38%	5.05%
poi 11	4.48%	9.77%	4.48%	12.71%	20.24%	9.05%	8.31%	23.81%	17.68%
poi 12	0.84%	0.00%	0.34%	0.04%	0.00%	0.00%	0.00%	0.00%	0.00%
poi 13	1.33%	1.15%	0.69%	0.83%	2.38%	2.67%	2.40%	2.38%	4.04%
poi 14	2.80%	2.30%	1.03%	7.80%	0.00%	0.00%	1.60%	0.00%	1.52%
poi 15	1.12%	1.15%	5.17%	1.50%	0.00%	1.44%	1.76%	4.76%	3.03%
Overall	1427	174	290	2525	84	486	626	42	198

Table 2: The input table for Figure 9.

Outputs	ST82	ST271	ST279	ST490	ST673	ST912	ST932	ST990	ST1077
vht 00	1.09%	1.19%	1.93%	1.92%	1.19%	0.77%	1.14%	0.73%	0.81%
vht 01	0.66%	0.54%	1.27%	1.45%	0.54%	0.44%	0.48%	0.52%	0.44%
vht 02	0.38%	0.30%	1.03%	0.95%	0.34%	0.16%	0.34%	0.40%	0.23%
vht 03	0.25%	0.21%	0.47%	0.61%	0.21%	0.10%	0.15%	0.09%	0.16%
vht 04	0.33%	0.32%	0.46%	0.51%	0.33%	0.19%	0.37%	0.16%	0.28%
vht 05	0.50%	0.49%	0.50%	0.48%	0.33%	0.53%	1.17%	0.21%	0.84%
vht 06	1.16%	1.11%	0.79%	0.92%	0.94%	1.15%	2.16%	0.63%	1.63%
vht 07	3.44%	2.50%	2.17%	2.93%	1.21%	2.48%	6.42%	1.18%	5.86%
vht 08	4.87%	3.41%	3.20%	4.11%	4.64%	3.28%	6.59%	2.04%	6.80%
vht 09	5.56%	4.40%	3.91%	4.42%	5.46%	4.80%	6.08%	3.84%	6.23%
vht 10	6.02%	4.60%	4.56%	4.47%	9.11%	5.00%	5.59%	5.15%	5.48%
vht 11	6.90%	3.95%	5.33%	4.84%	9.11%	6.38%	5.31%	7.53%	6.41%
vht 12	5.57%	3.76%	4.83%	4.30%	7.45%	5.43%	4.79%	6.97%	4.62%
vht 13	4.78%	4.43%	4.29%	4.31%	6.40%	4.56%	4.31%	5.97%	4.17%
vht 14	5.86%	5.27%	6.10%	6.13%	6.41%	5.16%	6.67%	8.08%	5.39%
vht 15	6.71%	5.51%	6.36%	6.16%	5.07%	5.53%	6.00%	8.23%	5.86%
vht 16	7.23%	5.48%	7.00%	6.56%	4.62%	10.95%	6.82%	10.19%	7.18%
vht 17	9.49%	6.88%	10.18%	9.04%	8.19%	12.09%	7.62%	10.12%	9.21%
vht 18	8.73%	8.10%	10.26%	9.00%	8.92%	8.67%	7.56%	9.70%	8.75%
vht 19	5.67%	7.19%	5.36%	5.18%	5.58%	5.29%	4.82%	5.41%	5.72%
vht 20	4.64%	9.05%	5.25%	5.39%	4.04%	5.57%	4.49%	3.14%	4.44%
vht 21	4.52%	10.78%	6.12%	6.26%	3.43%	5.76%	4.82%	3.08%	4.79%
vht 22	3.45%	6.49%	4.85%	5.64%	2.91%	3.61%	3.38%	1.77%	3.33%
vht 23	2.20%	3.82%	3.39%	3.74%	2.09%	1.84%	2.60%	1.95%	2.12%
Overall	541.36	23.84	582.38	579.24	18.99	23.66	109.62	22.33	64.20

Table 3: The forecast table for Figure 9.

While we have achieved excellent accuracy in the entire Haikou area in our previous accuracy experiments using ANNs in a randomly distributed geographic sample, cross-regional experiments using ANNs, RF, and SVM show extremely low accuracy when the models used for Haikou are applied to a larger-scale citywide area (Table 4). This is due to certain randomness in areas with sparse travel activity, a conclusion strengthened by

the accuracy visualizations (Figure 12). Samples with high error rates, marked with bright colors, in the accuracy images are always sparse in total VHT, which are shown as dark color in the ground truth images. As previously stated in the accuracy experiments, it is difficult for the algorithms to acquire irregular patterns from the data samples with sparse travel activity. Valid mapping relationships in these remote areas acquired by

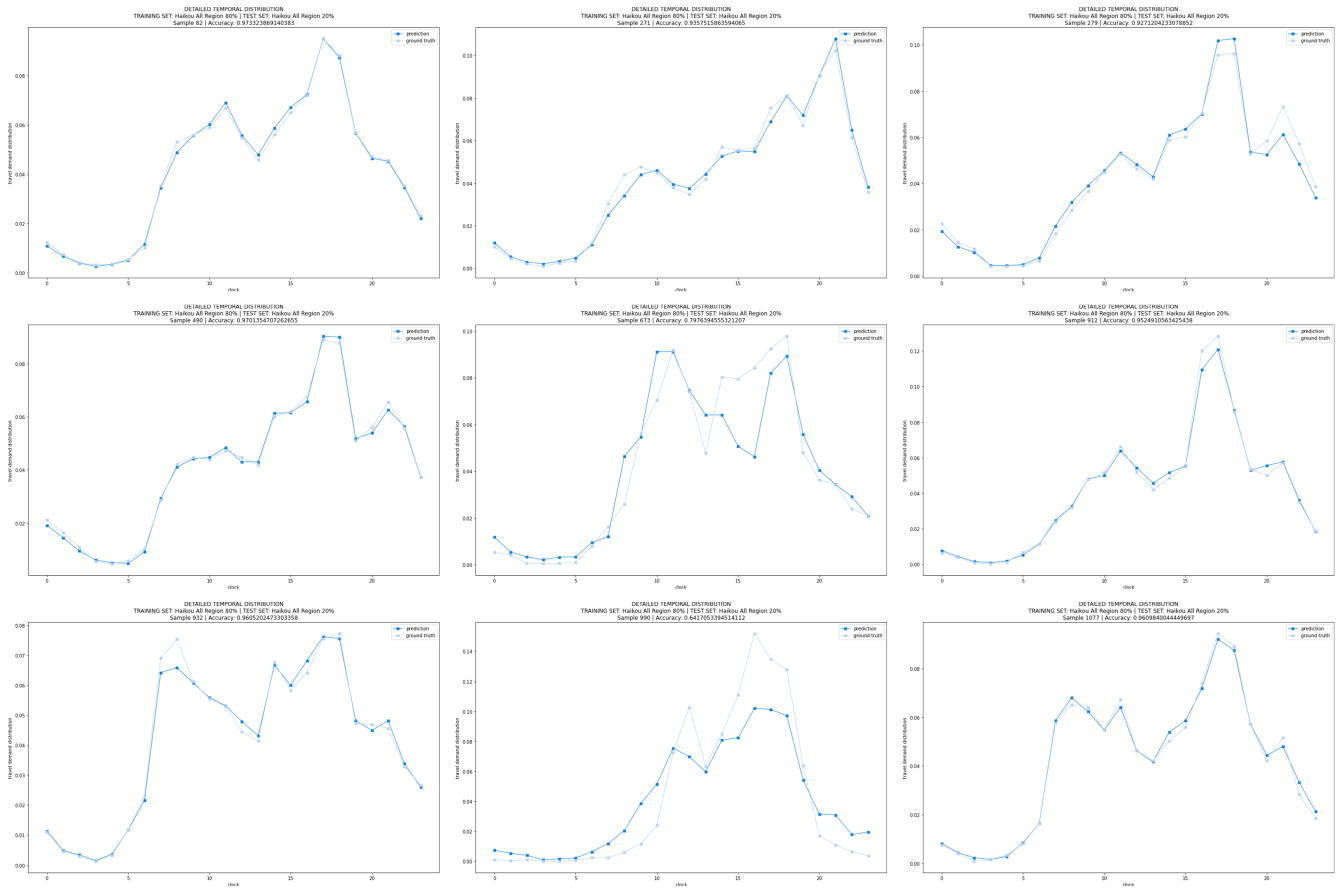


Figure 9: Instances of the prediction results (bright lines) calculated by our neural network are compared with the ground truths (faded lines).

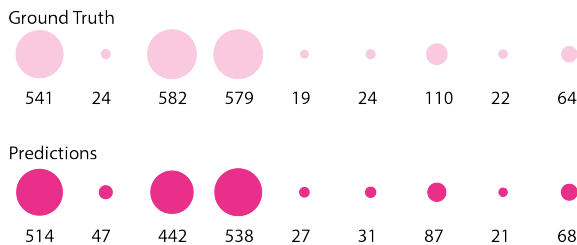


Figure 10: These circle areas represent the values of the ground truth or the prediction of daily average VHT taking place in nine samples (from left to right: ST82, ST271, ST279, ST490, ST673, ST912, ST932, ST990, ST1077).

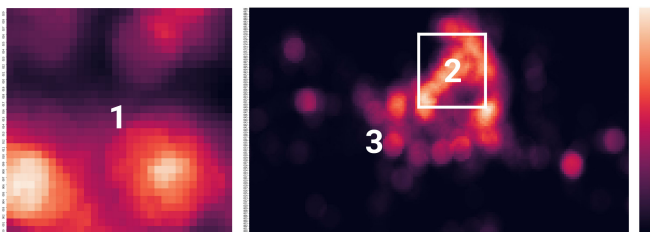


Figure 11: Urban function density map of the three different areas used in the accuracy test (2,3) and the multi-area hybrid test (1,2,3). (1: Chengdu Urban Area, 2: Haikou Urban Area, 3: the Entire Haikou)

the algorithms in areas with dense travel activity are also a challenge. In applying the model to an entire city area, the algorithm

overfitting occurs when exclusively trained on the urban center region.

Different computational models		Accuracy
ANNs	Haikou Urban	17.21%
	Chengdu Urban	33.35%
Linear SVR	Haikou Urban	-65.69%
	Chengdu Urban	-21.49%
Random Forest	Haikou Urban	-178.32%
	Chengdu Urban	-269.16%

Table 4: This table records the accuracy of VHT amount predictions in entire Haikou area.

	Model U→Set A	Model A→Set U
ANNs	36.10%	61.67%
Random Forest	30.12%	52.00%
Linear SVR	-65.68%	15.91%

Table 5: The all-region data set is divided into two parts, one of which (A) has monthly VHT accumulation above 2000 hours on each sample, the other (U) has monthly VHT accumulation under 2000 hours on each sample. This table shows the prediction accuracy of three algorithms between the two data sets.

Another experiment is conducted to illustrate the over-fitting phenomenon that transpires in citywide areas. The all-region dataset once again is divided into two parts. One contains

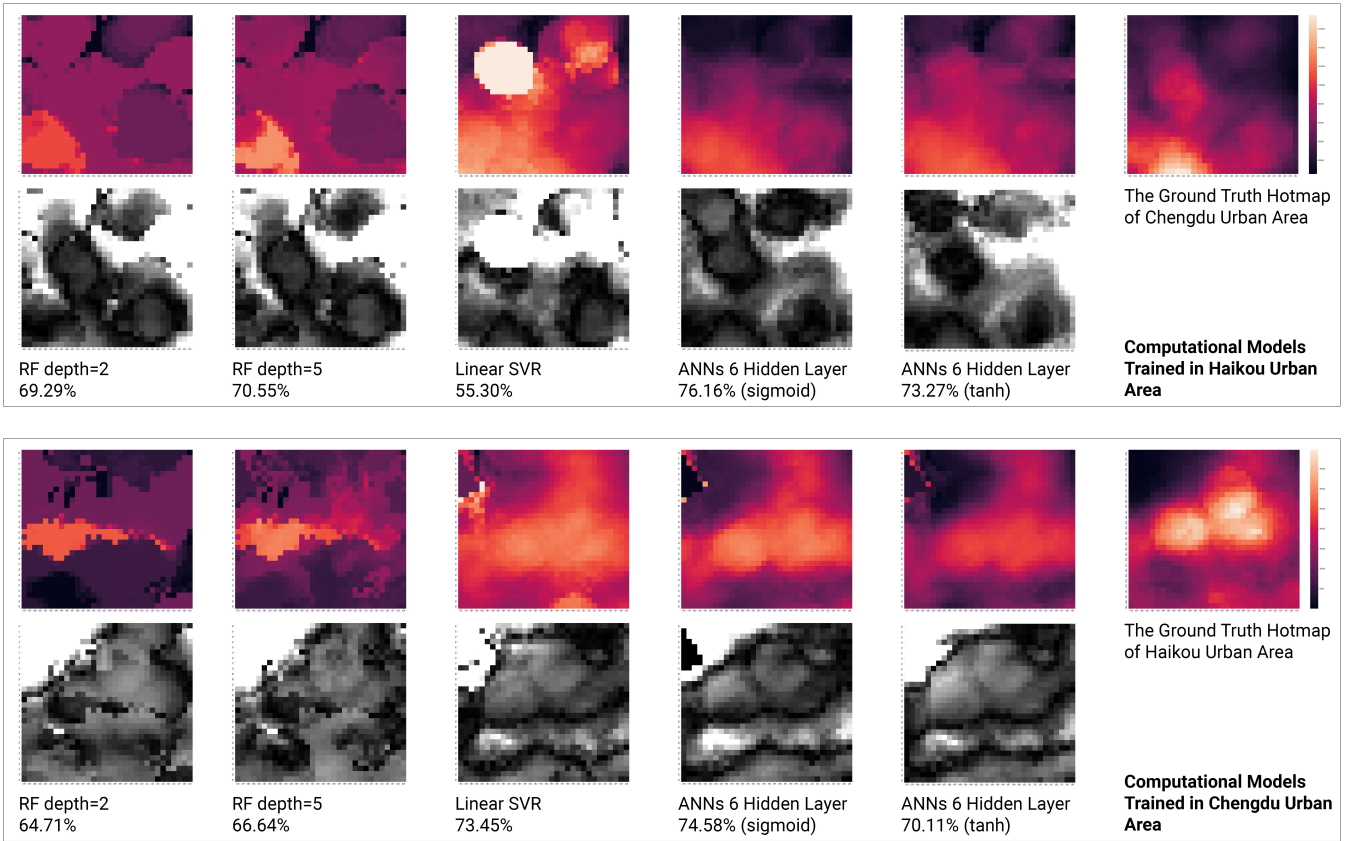


Figure 12: Accuracy and visualization of total vehicle travel demand in the cross-city experiments.

Different computational models		Accuracy of temporal distribution in different test areas		
		Haikou All-region	Haikou Urban	Chengdu Urban
ANNs	Haikou All-region	-	93.58%	80.04%
	Haikou Urban	83.47%	-	77.28%
	Chengdu Urban	77.05%	80.43%	-
Random Forest	Haikou All-region	-	89.31%	79.02%
	Haikou Urban	82.95%	-	75.79%
	Chengdu Urban	76.93%	78.19%	-
Linear SVR	Haikou All-region	-	91.34%	78.22%
	Haikou Urban	80.38%	-	73.74%
	Chengdu Urban	67.68%	76.50%	-

Table 6: This table records the accuracy results of temporal distribution in the cross-area experiment.

monthly VHT accumulation above 2000 hours on each sample. The other has a monthly VHT accumulation under 2000 hours. Using the multi-area test method, we tested the capability of three algorithms trained on one data set and then be applied on the other (Table 5). In reference to ANNs, the model of artificial neural network over-fits in the early stage of training according to the error rate curve (Figure 13), leading to the model of ANNs having an extremely low accuracy.

### 3.2.3. Temporal Distribution Forecasting

For a detailed VHT temporal distribution, the median accuracy values obtained in the experiments closely approach the

expected (Table 6) in both test region expansion and migration. The prediction accuracy of ANNs remains higher than that of SVM and RF. This is true in all the multi-area tests. According to the table 6, taking the multi-area test between urban areas of Chengdu and Haikou for example, the median accuracy reaches about 80% when the computational model is applied to a broader urban scale or the built environment of another urban area. It means that the prediction model has applicability among different urban environments, and the mapping relation acquired in one area can be reused elsewhere to a certain degree. To better demonstrate the accuracy of the prediction model's versatility, we selected and visualized three samples' tempo-

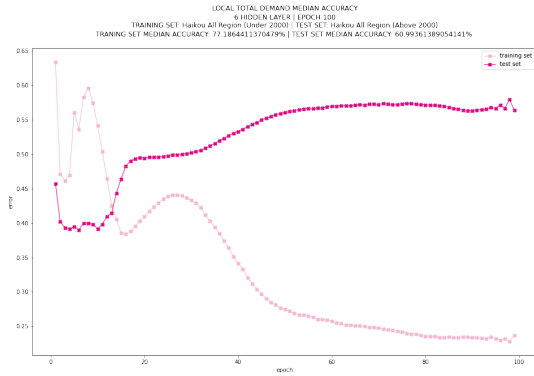


Figure 13: Over-fitting of ANNs in the prediction of the total VHT amount.

ral distribution predictions using all of Haikou as the training set and Chengdu environmental data as the input of the test process. The predictions of these three samples have similar patterns and the accuracy of them exceeds (85.54%), hovers around (81.22%), or strays below the median (74.22%) Figure 14). Compared with the richer patterns in figure 9, the model predicts a time distribution on these Chengdu samples close to real-time situations.

We have verified a link between our living environment and vehicle travel demand, which is consistent with previous studies of Cervero et al., and attempted to apply this relationship learned by the computational model in one area to a broader urban or other areas. Although there exist issues in predicting the total amount of VHT when applying computational models from congested city zones to fringes with scant activity, migration experiments have demonstrated the potential of applying models trained in one area to others. Thus, using this approach, the dataset from a limited number of areas can be utilized to map the relationship between living environment and vehicle travel demand. This will help urban researchers and designers in predicting detailed travel demand and offer feedback on improvements in the living environment, thus significantly reducing their upfront research costs.

### 3.3. AI-assisted Urban Design

In addition, we experimented with the final model results in terms of design applications. The final hybrid prediction model consists of a combination of ANNs with six and seven hidden layers for predicting, respectively, the amount of vehicle travel demand and the related temporal distribution. As stated previously, a large body of prior research showed that mixed land use can promote non-vehicular traveling and thus reduce demand. However, the extent and specific effects of functional mixing are vague in most studies. Without such references, designers struggle to intuitively and quickly obtain feedback on functional blends. To demonstrate the value of our approach in this scenario, hybrid computational models are used in this study to explore a novel design approach.

We selected and adjusted the urban functions of the buffer areas near four sample points: Nanda Overpass (110.3303, 20.0199), Haikou People’s Park (110.3392, 20.0363), Haikou

East Railway Station (110.3382, 19.9854), and Hainan Government (110.3441, 20.0207). Four different types of urban functions are focused in the study related to the choice of travel patterns: restaurants, residential areas, workplaces, and public transportation. In addition, we endeavored to predict the case where the original function ratios are maintained while the density thereof increases, including where the number of urban functions is the same for all types (i.e., the case where the entropy of the urban function mix is highest). The table 7 records our inputs for seven different functional ratios, including the original functional numbers, at four locations. Simultaneously, the figure 15 records the outputs of our hybrid computational model for predicting vehicle travel demand in these modified living environments. Notably, the designer must interpret the results as associative because the link between living environment and travel demand learned by the computational model is not causal in nature.

The conclusion that can be drawn from the figure 15 is that a perfectly average distribution of functions does not imply an optimal distribution of traffic demand. It is a possibility that the largest entropy in a mix of urban functions begets an even more irrational distribution of traffic demand. The green line in the figure represents numerical uniformity in all the functions, and peak traffic demand not only stagnates but indeed could increase. This again illustrates the potential for misleading conclusions to be drawn from vaguely describing information in the urban environment. Conversely, among the adjustment measures for the four explicit functional categories, the approach with a clear effect involves mainly public transport. A reduction of traffic pressure in all four locations can be notably observed when public transport stations increase. At the same time, an increase of residential functions for the peak traffic periods depends on the situation. Adding residential block modules near Haikou People’s Park corresponds to the relief of traffic pressure. Similar measures performed near East Station instead correspond to higher traffic demand.

### 3.4. Combined with Genetic Algorithm

Further, we embed the trained model into a genetic algorithm. The combination of genetic algorithms and predictive models (Figure 16) help discover the optimal or near-optimal solution for our living environment under a specific travel distribution objective. Firstly, a group of urban functional ratios that satisfy the initial constraints is created randomly. Individual objects are entered into a hybrid ANNs model and output predictions, and further evaluations are performed to derive a metric related to travel demand. Referring to this metric as the fitness, the best group of individual objects representing the built environment is selected and subsequently reassessed. The cycle of evaluation, selection, and derivation operations repeats until an optimal or near-optimal solution arrives.

Urban decision-makers can set the desired travel demand for a certain urban area or period to solve problems such as the temporal distribution of transportation resources, which might require optimizing the ratios of urban functions within a range for a specific location. In a practical sense, that involves mixing

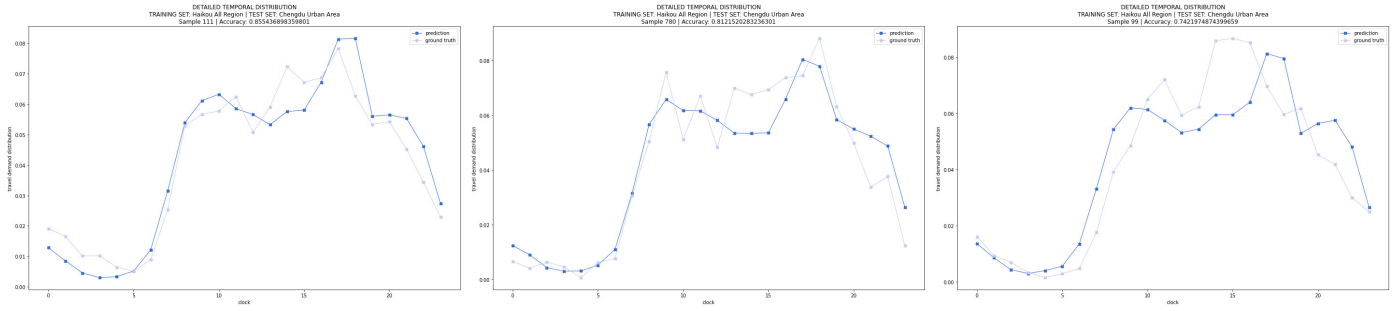


Figure 14: The output instances of prediction model which uses the same training set as figure 9 but is tested in Chengdu

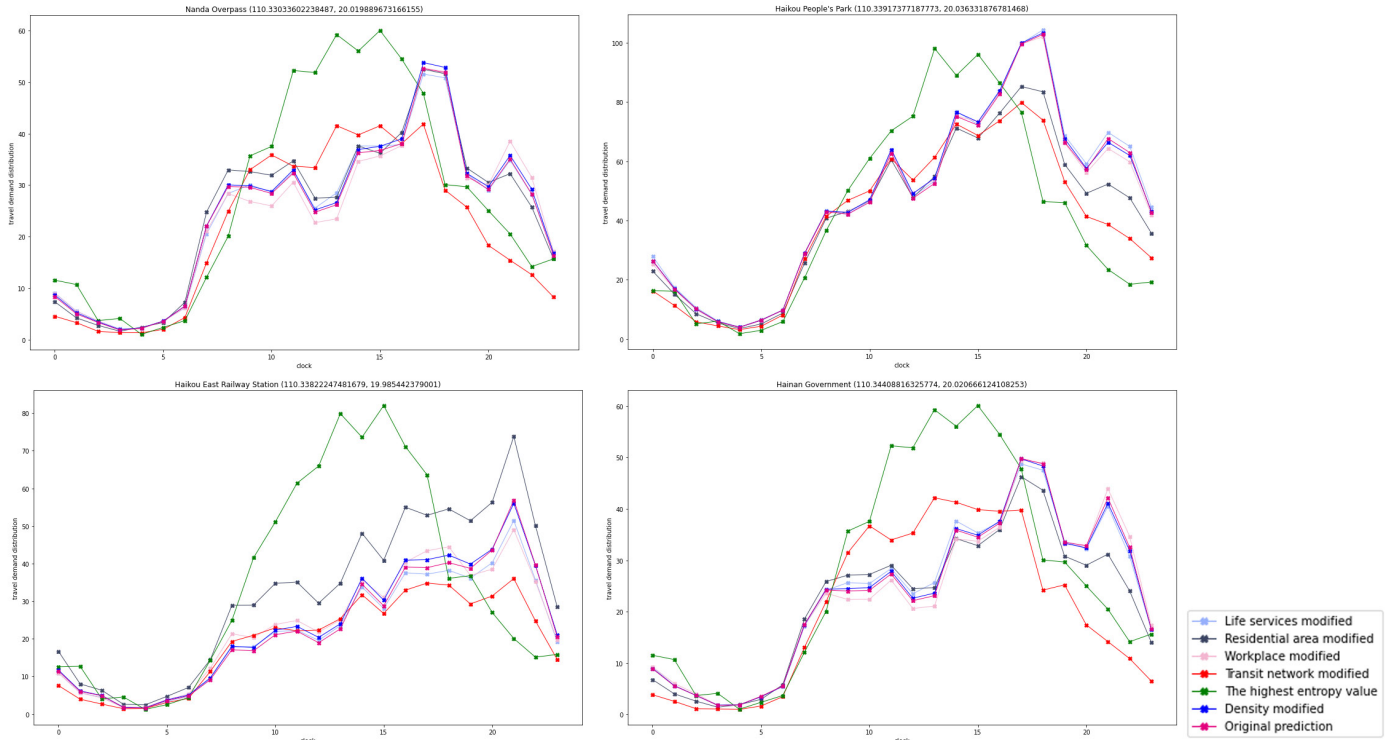


Figure 15: The output instances of prediction model which uses the same training set as figure 9 but is tested in Chengdu

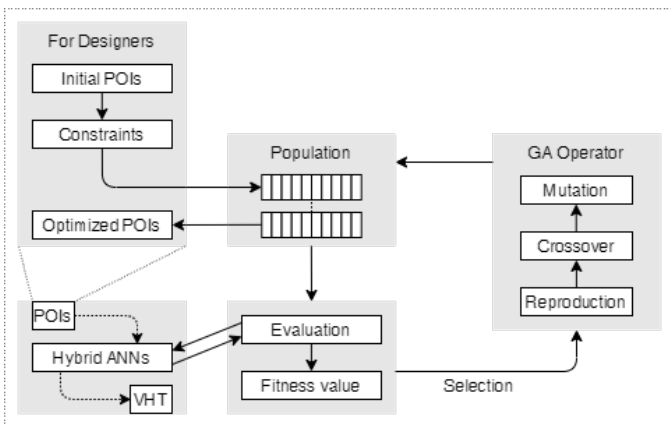


Figure 16: the combination of genetic algorithms and hybrid ANNs

nities at the proper scale to solve the problem of traffic peaks in job to home.

With some locations of interest, the functional ratios in the built environment are used as individual objects for optimization by the genetic algorithm under certain constraints and objectives set by the “designer.” The predictive model or its variants are used as the fitness function to optimize the functional ratios.

Using Haikou People’s Park as an example, the number of total urban function interest points and type-12 (transportation hub) remain unchanged. The remaining interest points vary up or down by 50 based on the current number, and all are greater than or equal to 0. The objective function is to minimize the variance of vehicle travel demand at different periods to optimize the invocation of transportation resources and release the traffic pressure during peak periods. After the iterative process of the genetic algorithm, the designer can obtain the optimized results as shown in the figure 17 (light blue line). Indeed, the

residential and office areas to construct self-contained commu-

Nanda Overpass																	
POI	00	01	02	03	04	05	06	07	08	09	10	11	12	13	14	15	sum
1	88	19	10	18	72	103	112	3	122	44	108	71	0	27	90	16	904
2	88	35	26	34	88	119	112	3	122	44	108	71	0	27	90	16	984
3	88	19	10	18	72	103	112	3	202	44	108	71	0	27	90	16	984
4	88	19	10	18	72	103	112	3	122	84	128	91	0	27	90	16	984
5	88	19	10	18	72	103	112	3	122	44	108	71	0	107	90	16	984
6	-	-	-	-	-	-	-	-	-	-	-	-	-	-	-	-	984
7	95	20	10	19	78	112	121	3	133	47	117	77	0	29	97	17	984

Haikou People's Park																	
POI	00	01	02	03	04	05	06	07	08	09	10	11	12	13	14	15	sum
1	40	191	86	178	168	247	214	32	205	259	254	284	0	27	118	102	2405
2	40	207	102	194	184	263	214	32	205	259	254	284	0	27	118	102	2485
3	40	191	86	178	168	247	214	32	285	259	254	284	0	27	118	102	2485
4	40	191	86	178	168	247	214	32	205	299	274	304	0	27	118	102	2485
5	40	191	86	178	168	247	214	32	205	259	254	284	0	107	118	102	2485
6	-	-	-	-	-	-	-	-	-	-	-	-	-	-	-	-	2485
7	41	197	88	183	173	255	221	33	211	267	262	293	0	27	121	105	2485

Haikou East Railway Station																	
POI	00	01	02	03	04	05	06	07	08	09	10	11	12	13	14	15	sum
1	82	498	157	488	50	74	106	5	106	102	41	114	2	15	23	13	1876
2	82	514	173	504	66	90	106	5	106	102	41	114	2	15	23	13	1956
3	82	498	157	488	50	74	106	5	186	102	41	114	2	15	23	13	1956
4	82	498	157	488	50	74	106	5	106	142	61	134	2	15	23	13	1956
5	82	498	157	488	50	74	106	5	106	102	41	114	2	95	23	13	1956
6	-	-	-	-	-	-	-	-	-	-	-	-	-	-	-	-	1956
7	85	519	163	508	52	77	110	5	110	106	42	118	2	15	23	13	1956

Hainan Government																	
POI	00	01	02	03	04	05	06	07	08	09	10	11	12	13	14	15	sum
1	50	16	21	50	65	66	87	8	87	166	96	75	0	15	83	24	909
2	50	32	37	66	81	82	87	8	87	166	96	75	0	15	83	24	989
3	50	16	21	50	65	66	87	8	167	166	96	75	0	15	83	24	989
4	50	16	21	50	65	66	87	8	87	206	116	95	0	15	83	24	989
5	50	16	21	50	65	66	87	8	87	166	96	75	0	95	83	24	989
6	-	-	-	-	-	-	-	-	-	-	-	-	-	-	-	-	989
7	54	17	22	54	70	71	94	8	94	180	104	81	0	16	90	26	989

Table 7: The input table for Figure 15. This table records the attempts of urban function adjustment using the computational model under four urban locations. (Columns 00 to 15 annotate the number of 16 urban function types in Table 8 as input of each attempt; rows 1 to 7 indicate: numbers of original functions, numbers after adjustment of shopping-related urban functions, adjustment of residential areas, adjustment of workplace-related urban functions, adjustment of public transportation-related urban functions such as bus station, and the case making the number of all types of functions mutually equal to each other, the case maintaining the original proportion of functions)

peak of travel demand can be relieved with the new urban function ratio.

In addition, although invoking the trained ANNs model for each prediction takes  $525 \text{ ms} \pm 6.41 \text{ ms}$ , the genetic algorithm performs many operations, and the process can take up to several hours. The designer can place additional constraints to better fit the actual situation and significantly reduce the optimization time of the genetic algorithm. For example, the designer can set four further base parameters weighted to determine the amount of variation in the four POI categories of eating, housing, work, and public transportation. They can subsequently optimize these four parameters in the genetic algorithm instead of optimizing all 16 POI quantity parameters to conserve time. The figure 17 also contains the results of this more constrained

optimization (dark blue line), which also maps out a more reasonable travel demand time variation with a lower peak than the original one (magenta line). The proposed POI ratios (dark blue columns) derived from this approach are less modified for the built environment. In the case demonstrated here, all functional categories remain largely unchanged except for residential density, which should be increased.

#### 4. Conclusion and Further Study

Past research revealed an intrinsic link between land use and travel demand, which helped designers consider urban functional planning from a new perspective. However, there lacked a proper methodology allowing the ability designers to obtain

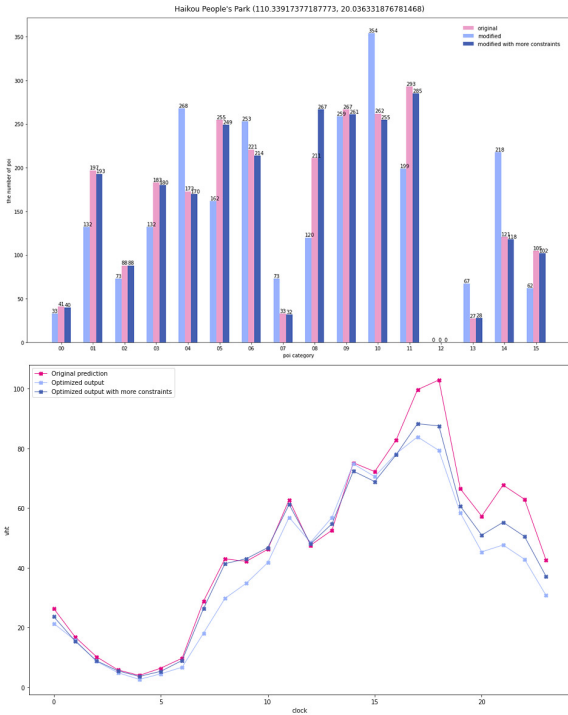


Figure 17: The optimized result in Haikou People's Park

## 5. Appendix

Index	Building Function
00	automobile and motorcycle related
01	food and beverages related
02	shopping related place
03	daily life service place
04	sports and recreation place
05	medical and health care service place
06	accommodation service related
07	tourist attraction related
08	residential area
09	enterprise
10	governmental and social groups related
11	science and education cultural place
12	traffic hinge
13	transit network
14	finance and insurance service institution
15	public facility

Table 8: Urban Function Category According to AutoNavi

detailed travel demand predictions and clear recommendations for urban planning adjustments. Also, the methodology of past studies resulted in a lack of a sufficient basis to migrate findings between different regions.

Meanwhile, the emergence of machine learning and big data created a new paradigm of urban research, and several studies utilized machine learning models to enhance traditional workflow and take a more detailed analysis and prediction of traditional urban problems. Our research develops a new computational model to map the relationship between built environments and travel demand, thus creating a network of feedback in the urban planning and design process. The study shows how computational models can be adapted and trained to accurately predict the relationship between an array representing the built environment and vehicle travel demand. The accuracy and transferability of the computational models are further proven to be feasible. With the trained model, we can accurately predict the vehicle travel demand that may occur at a location at various times.

With this prediction model, designers can establish explicit urban function compositions as the input and make predictions to obtain a detailed vehicle travel demand profile including total amount and its time distribution. In addition, we show separately in our application exploration how the designer can adjust the inputs to obtain feedback and further leverage the genetic algorithm to obtain explicit suggestions for city function adjustment with the expected travel demand target. In addition, other factors such as socio-economic and policy factors can also affect traffic behavior and travel demand (Forsyth et al., 2008; McNally and Kulkarni, 1997). In future studies, we aim to quantify these behaviors.

## References

- Arentze, T., Hofman, F., Van Mourik, H., Timmermans, H., and Wets, G. (2000). Using decision tree induction systems for modeling space-time behavior. *Geographical analysis*, 32(4):330–350.
- Bao, J., Yu, H., and Wu, J. (2019). Short-term ffb demand prediction with multi-source data in a hybrid deep learning framework. *IET Intelligent Transport Systems*, 13(9):1340–1347.
- Basheer, I. A. and Hajmeer, M. (2000). Artificial neural networks: fundamentals, computing, design, and application. *Journal of microbiological methods*, 43(1):3–31.
- Cervero, R. (1989). Land-use mixing and suburban mobility.
- Cervero, R. (1991). Land uses and travel at suburban activity centers.
- Cervero, R. (1994). Transit-based housing in california: evidence on ridership impacts. *Transport Policy*, 1(3):174–183.
- Cervero, R. (1996). Mixed land-uses and commuting: Evidence from the american housing survey. *Transportation Research Part A: Policy and Practice*, 30(5):361–377.
- Cervero, R. and Duncan, M. (2003). Walking, bicycling, and urban landscapes: evidence from the san francisco bay area. *American journal of public health*, 93(9):1478–1483.
- Cervero, R. and Duncan, M. (2006). 'which reduces vehicle travel more: Jobs-housing balance or retail-housing mixing? *Journal of the American planning association*, 72(4):475–490.
- Cervero, R. and Kockelman, K. (1997). Travel demand and the 3ds: Density, diversity, and design. *Transportation research part D: Transport and environment*, 2(3):199–219.
- Chauhan, S., Agarwal, N., and Kar, A. K. (2016). Addressing big data challenges in smart cities: a systematic literature review. *info*.
- Choi, D., Kang, M., and Yoon, J. (2021). Utility of mixed-use development by reducing aggregated travel time for multiple non-work activities: A case of seoul, korea. *Cities*, 109:103007.
- Clifton, K., Ewing, R., Knaap, G.-J., and Song, Y. (2008). Quantitative analysis of urban form: a multidisciplinary review. *Journal of Urbanism*, 1(1):17–45.
- Davis, N., Raina, G., and Jagannathan, K. (2016). A multi-level clustering approach for forecasting taxi travel demand. In *2016 IEEE 19th International Conference on Intelligent Transportation Systems (ITSC)*, pages 223–228. IEEE.

- Demir, I., Koperski, K., Lindenbaum, D., Pang, G., Huang, J., Basu, S., Hughes, F., Tuija, D., and Raskar, R. (2018). Deepglobe 2018: A challenge to parse the earth through satellite images. In *Proceedings of the IEEE Conference on Computer Vision and Pattern Recognition Workshops*, pages 172–181.
- Downs, A. (2005). *Still stuck in traffic: coping with peak-hour traffic congestion*. Brookings Institution Press.
- Dunphy, R. T. and Fisher, K. (1996). Transportation, congestion, and density: new insights. *Transportation Research Record*, 1552(1):89–96.
- Ewing, R. and Cervero, R. (2001). Travel and the built environment: a synthesis. *Transportation research record*, 1780(1):87–114.
- Ewing, R. and Cervero, R. (2010). Travel and the built environment: A meta-analysis. *Journal of the American planning association*, 76(3):265–294.
- Feng, C. and Jiao, J. (2021). Predicting and mapping neighborhood-scale health outcomes: A machine learning approach. *Computers, Environment and Urban Systems*, 85:101562.
- Forsyth, A., Hearst, M., Oakes, J. M., and Schmitz, K. H. (2008). Design and destinations: factors influencing walking and total physical activity. *Urban studies*, 45(9):1973–1996.
- Frank, L. D., Andresen, M. A., and Schmid, T. L. (2004). Obesity relationships with community design, physical activity, and time spent in cars. *American journal of preventive medicine*, 27(2):87–96.
- Frank, L. D., Schmid, T. L., Sallis, J. F., Chapman, J., and Saelens, B. E. (2005). Linking objectively measured physical activity with objectively measured urban form: findings from smartraq. *American journal of preventive medicine*, 28(2):117–125.
- Gervasoni, L., Bosch, M., Fenet, S., and Sturm, P. (2016). A framework for evaluating urban land use mix from crowd-sourcing data. In *2016 IEEE International Conference on Big Data (Big Data)*, pages 2147–2156. IEEE.
- Grekousis, G., Manetos, P., and Photis, Y. N. (2013). Modeling urban evolution using neural networks, fuzzy logic and gis: The case of the athens metropolitan area. *Cities*, 30:193–203.
- Hadjimichael, A., Comas, J., and Corominas, L. (2016). Do machine learning methods used in data mining enhance the potential of decision support systems? a review for the urban water sector. *Ai Communications*, 29(6):747–756.
- Hancke, G. P., Hancke Jr, G. P., et al. (2013). The role of advanced sensing in smart cities. *Sensors*, 13(1):393–425.
- Ibrahim, M. R., Haworth, J., and Cheng, T. (2020). Understanding cities with machine eyes: A review of deep computer vision in urban analytics. *Cities*, 96:102481.
- Kandrika, S. and Roy, P. S. (2008). Land use land cover classification of orissa using multi-temporal irs-p6 awifs data: A decision tree approach. *International Journal of Applied Earth Observation and Geoinformation*, 10(2):186–193.
- Kang, C., Shi, L., Wang, F., and Liu, Y. (2020). How urban places are visited by social groups? evidence from matrix factorization on mobile phone data. *Transactions in GIS*, 24(6):1504–1525.
- Karsoliya, S. (2012). Approximating number of hidden layer neurons in multiple hidden layer bpnn architecture. *International Journal of Engineering Trends and Technology*, 3(6):714–717.
- Li, W., Wang, S., Zhang, X., Jia, Q., and Tian, Y. (2020). Understanding intra-urban human mobility through an exploratory spatiotemporal analysis of bike-sharing trajectories. *International Journal of Geographical Information Science*, 34(12):2451–2474.
- Liu, L., Silva, E. A., Wu, C., and Wang, H. (2017). A machine learning-based method for the large-scale evaluation of the qualities of the urban environment. *Computers, environment and urban systems*, 65:113–125.
- Liu, X., Sun, L., Sun, Q., and Gao, G. (2020). Spatial variation of taxi demand using gps trajectories and poi data. *Journal of Advanced Transportation*, 2020.
- Liu, Y., Wang, F., Xiao, Y., and Gao, S. (2012). Urban land uses and traffic ‘source-sink areas’: Evidence from gps-enabled taxi data in shanghai. *Landscape and Urban Planning*, 106(1):73–87.
- Loh, W.-Y. (2011). Classification and regression trees. *Wiley interdisciplinary reviews: data mining and knowledge discovery*, 1(1):14–23.
- Loudon, W. R., Ruiters, E. R., and Schlappi, M. L. (1988). *Predicting Peak-Spreading Under Congested Conditions*. Number 1203.
- Maharana, A. and Nsoesie, E. O. (2018). Use of deep learning to examine the association of the built environment with prevalence of neighborhood adult obesity. *JAMA network open*, 1(4):e181535–e181535.
- Maria Kockelman, K. (1997). Travel behavior as function of accessibility, land use mixing, and land use balance: evidence from san francisco bay area. *Transportation research record*, 1607(1):116–125.
- McCauley, S. and Goetz\*, S. (2004). Mapping residential density patterns using multi-temporal landsat data and a decision-tree classifier. *International Journal of Remote Sensing*, 25(6):1077–1094.
- McNally, M. G. and Kulkarni, A. (1997). Assessment of influence of land use–transportation system on travel behavior. *Transportation Research Record*, 1607(1):105–115.
- Nosratabadi, S., Mosavi, A., Keivani, R., Ardabili, S., and Aram, F. (2019). State of the art survey of deep learning and machine learning models for smart cities and urban sustainability. In *International Conference on Global Research and Education*, pages 228–238. Springer.
- Park, K., Ewing, R., Scheer, B. C., and Tian, G. (2018). The impacts of built environment characteristics of rail station areas on household travel behavior. *Cities*, 74:277–283.
- Sabouri, S., Brewer, S., and Ewing, R. (2020). Exploring the relationship between ride-sourcing services and vehicle ownership, using both inferential and machine learning approaches. *Landscape and Urban Planning*, 198:103797.
- Sallis, J. F., Cerin, E., Conway, T. L., Adams, M. A., Frank, L. D., Pratt, M., Salvo, D., Schipperijn, J., Smith, G., Cain, K. L., et al. (2016). Physical activity in relation to urban environments in 14 cities worldwide: a cross-sectional study. *The lancet*, 387(10034):2207–2217.
- Shallal, L. and Khan, A. (1980). Predicting peak-hour traffic. *Traffic Quarterly*, 34(1).
- Shen, Y. and Karimi, K. (2016). Urban function connectivity: Characterisation of functional urban streets with social media check-in data. *Cities*, 55:9–21.
- Song, Y., Merlin, L., and Rodriguez, D. (2013). Comparing measures of urban land use mix. *Computers, Environment and Urban Systems*, 42:1–13.
- Souza, J. T. d., Francisco, A. C. d., Piekarski, C. M., and Prado, G. F. d. (2019). Data mining and machine learning to promote smart cities: A systematic review from 2000 to 2018. *Sustainability*, 11(4):1077.
- Systematics, C., Deakin, Skabardonis, H., Administration, U. S. F. T., of Transportation, U. S. D., and (US), T. S. P. (1994). *The effects of land use and travel demand management strategies on commuting behavior*. US Department of Transportation.
- Tong, Y., Chen, Y., Zhou, Z., Chen, L., Wang, J., Yang, Q., Ye, J., and Lv, W. (2017). The simpler the better: a unified approach to predicting original taxi demands based on large-scale online platforms. In *Proceedings of the 23rd ACM SIGKDD international conference on knowledge discovery and data mining*, pages 1653–1662.
- Vlahogianni, E. I., Kepaptsoglou, K., Tsetos, V., and Karlaftis, M. G. (2016). A real-time parking prediction system for smart cities. *Journal of Intelligent Transportation Systems*, 20(2):192–204.
- Wachs, M. (1989). Regulating traffic by controlling land use the southern california experience. *Transportation*, 16(3):241–256.
- Wang, M. and Debbage, N. (2021). Urban morphology and traffic congestion: Longitudinal evidence from us cities. *Computers, Environment and Urban Systems*, 89:101676.
- Wets, G., Vanhoof, K., Arentze, T., and Timmermans, H. (2000). Identifying decision structures underlying activity patterns: an exploration of data mining algorithms. *Transportation Research Record*, 1718(1):1–9.
- Yamamoto, T., Kitamura, R., and Fujii, J. (2002). Drivers’ route choice behavior: analysis by data mining algorithms. *Transportation Research Record*, 1807(1):59–66.
- Yao, Y., Li, X., Liu, X., Liu, P., Liang, Z., Zhang, J., and Mai, K. (2017). Sensing spatial distribution of urban land use by integrating points-of-interest and google word2vec model. *International Journal of Geographical Information Science*, 31(4):825–848.
- Youssef, R., Aniss, M., and Jamal, C. (2020). Machine learning and deep learning in remote sensing and urban application: A systematic review and meta-analysis. In *Proceedings of the 4th Edition of International Conference on Geo-IT and Water Resources 2020, Geo-IT and Water Resources 2020*, pages 1–5.
- Yuan, J., Zheng, Y., and Xie, X. (2012). Discovering regions of different functions in a city using human mobility and pois. In *Proceedings of the 18th ACM SIGKDD international conference on Knowledge discovery and data mining*, pages 186–194.
- Yue, Y., Zhuang, Y., Yeh, A. G., Xie, J.-Y., Ma, C.-L., and Li, Q.-Q. (2017). Measurements of poi-based mixed use and their relationships with neigh-

- bourhood vibrancy. *International Journal of Geographical Information Science*, 31(4):658–675.
- Zhang, S., Tang, J., Wang, H., Wang, Y., and An, S. (2017). Revealing intra-urban travel patterns and service ranges from taxi trajectories. *Journal of Transport Geography*, 61:72–86.
- Zhao, P., Kwan, M.-P., and Zhou, S. (2018). The uncertain geographic context problem in the analysis of the relationships between obesity and the built environment in guangzhou. *International journal of environmental research and public health*, 15(2):308.